A Consistent Boltzmann Algorithm

Francis J. Alexander, Alejandro L. Garcia,* and Berni J. Alder
Lawrence Livermore National Laboratory, Livermore, California 94550
(Received 14 February 1995)

The direct simulation Monte Carlo method for the Boltzmann equation is modified by an additional displacement in the advection process and an enhanced collision rate in order to obtain the exact hard sphere equation of state at all densities. This leads to consistent thermodynamic and transport properties in the low density (Boltzmann) regime. At higher densities transport properties are comparable to the predictions of the Enskog model. The algorithm is faster than molecular dynamics at low and moderate densities and readily run on a parallel architecture.

PACS numbers: 05.70.Ce, 02.50.Ng, 51.10.+y

The direct simulation Monte Carlo (DSMC) method is a particle-based, numerical scheme for solving the nonlinear Boltzmann equation for hard spheres (HS) [1–3]. Rather than exactly calculating successive HS collisions, as in molecular dynamics (MD) [4], DSMC generates collisions stochastically with scattering rates and postcollision velocity distributions determined from the kinetic theory of a dilute HS gas. DSMC encounters the usual inconsistency of the Boltzmann equation; namely, it yields the transport properties for a dilute HS gas with diameter σ, yet has an *ideal gas* equation of state (implying $\sigma = 0$) [5]. In this Letter a modification to DSMC is introduced which removes this inconsistency and recovers the exact HS equation of state at *all* densities with virtually no additional computational cost. This consistent Boltzmann algorithm (CBA) has transport properties that are in similar (in some cases better) agreement with HS MD than Enskog theory [6].

In the standard DSMC method the positions and velocities $\{\vec{r}_i, \vec{v}_i\}$ of the particles (mass m) are evolved in time by two steps: advection and collisions. During the advection step all particles are simultaneously propagated a distance $\vec{v}_i \delta t$, where the time step δt is typically on the order of the mean collision time. The particles are sorted into (fixed) spatial cells of dimension δx, which is typically on the order of λ, the mean free path. Within each cell pairs of particles are then randomly selected as possible collision partners with a HS collision probability that is dependent on their relative velocities. Once a pair is selected, the postcollision relative velocities are also stochastically determined, consistent with the conservation of momentum and energy. The collision is executed with the particles remaining in place.

Since in the Boltzmann equation the advection process corresponds to that of point particles, the virial $\Theta = \langle \Delta \vec{v}_i \cdot \vec{r}_{ij} \rangle$ is zero, giving an ideal gas equation of state ($\Delta \vec{v}_i$ is the change in velocity of particle i, and $\vec{r}_{ij}$ is the line connecting the centers of the colliding particles). To obtain the correct HS virial, the CBA includes the extra displacement in the advection step that the particles would have experienced if they had collided as hard spheres [7],

$$\vec{d} = \frac{\vec{v}_r' - \vec{v}_r}{|\vec{v}_r' - \vec{v}_r|}\,\sigma\,, \tag{1}$$

where $\vec{v}_r = \vec{v}_1 - \vec{v}_2$ and $\vec{v}_r' = \vec{v}_1' - \vec{v}_2'$ are the precollision and postcollision relative velocities, respectively [8]. Particle 1 is displaced by the vector distance $\vec{d}$ and particle 2 by $-\vec{d}$, as shown in Fig. 1. Equation (1) implies that in a one-dimensional system, when two hard rods of length σ collide, that after the collision the distance between centers will be larger than the separation between similarly colliding point particles by a distance 2σ [9]. For hard spheres in three dimensions this effect generalizes to the displacement $\vec{d}$ above. In the low density limit the displacement yields the HS second virial coefficient $b_2 = (2\pi/3)\,\sigma^3$ and hence consistency.

At higher densities the collision rate, Γ, in a HS gas is enhanced due to the volume occupied by the spheres [6]; $\Gamma = \Lambda Y$, where Λ is the Boltzmann (i.e., low density) collision rate. These are, of course, functions of n, the number density; the Y factor is known from Monte Carlo and MD simulations. When the collision rate Γ is used in the CBA, the correct virial and hence, equation of state, is obtained at all densities.

Kinetic theory calculations and a series of computer simulations were carried out to obtain quantitative results from this model. Pressure measured by the normal momentum transfer across a plane confirmed that the

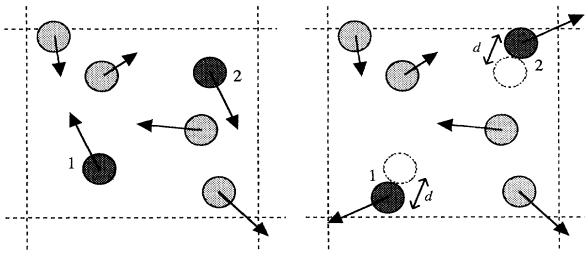

FIG. 1. Schematic illustration of the displacement occurring after a collision.

 0031-9007/95/74(26)/5212(4)$06.00

simulation reproduced the HS equation of state. From the hydrodynamic expression for the direct scattering function, $S(k, \omega)$, the sound speed obtained from the location of the Brillouin peak is in agreement with HS MD at low densities. At higher densities the Rayleigh and Brillouin peaks are not well separated. Thus, accurate measurements of the sound speed cannot be made in this way. The radial distribution (pair correlation) function is that of a perfect gas, so the sound speed determined from the equal-time density fluctuations (via the compressibility) is not in agreement with the correct value obtained directly from the equation of state.

The transport coefficients, namely, the shear viscosity (η), thermal conductivity (κ), and self-diffusion (D), have been measured numerically as well as determined analytically from their kinetic theory expressions [10,11]. They are of the Enskog form; that is, there are three separate contributions to the total transport coefficient—a kinetic (K), a potential (P), and a kinetic-potential cross (C) term. For example, for the viscosity,

$$\eta/\eta_0 = \frac{\eta^K}{Y} + \eta^C b_2 n + \eta^P (b_2 n)^2 Y, \qquad (2)$$

where η_0 is the shear viscosity in the low density (Boltzmann) approximation. The kinetic and cross contributions are identical to those given by Enskog theory [6]. Specifically, $\eta^K = 1$, $\kappa^K = 1$, $D^K = 1$, $\eta^C = 4/5$, $\kappa^K = 6/5$, and $D^C = 0$. The potential contributions must also be of the Enskog form; for example, for the viscosity,

$$\eta^P = A + B \int_0^\infty \exp(-st)\, dt, \qquad (3)$$

where t is measured in units of the mean collision time. The term A represents the delta function contribution from the initial displacement ($t = 0$) and is proportional to the Boltzmann average of the displacement squared for diffusion, of the momentum flux squared for viscosity, and of the energy flux squared for thermal conductivity. The coefficient B is proportional to the initial decay in the autocorrelation function determined from the next collision in which a common particle participates. The integral has the usual representation of a Markov process [10,11], where the exponential s represents the decay of correlations with further stochastic collisions.

CBA calculations for the shear viscosity yield $A = 144/25\pi$, or 3 times its Enskog value, and for the thermal conductivity, $A = 64/25\pi$, or twice its Enskog value. For shear viscosity, $B = -32/25(3\sqrt{3} + \pi) \approx -0.1535$, or -1.28 times its Enskog value, and for thermal conductivity (numerically) $B = 0.104 \pm 0.004$, or 0.559 ± 0.022 times its Enskog value. Previous work [11] has shown that the decay constant s, for the potential term is the same as the decay constant for the kinetic and cross terms, namely, $s = 4/5$ for shear viscosity, and $s = 8/15$ for thermal conductivity. This leads to a potential contribution to η^P of 1.64 or 2.15 times the Enskog result and a potential contribution to κ^P of 1.01 ± 0.01 or 1.34 ± 0.01 times the Enskog result. In these calculations the artificial contribution to momentum and energy transfer due to the finite distance separation between colliding particles within the same cell has been eliminated.

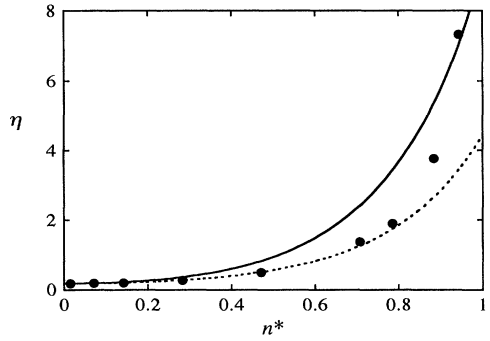

FIG. 2. HS shear velocity as a function of number density (with $kT = m = \sigma = 1$, $n^* = n\sigma^3$). The solid curve represents CBA, the dashed curve Enskog theory, and the solid circles HS MD (from [11]).

The shear viscosity measured in nonequilibrium flows (Poiseuille and relaxing velocity sine wave) was in agreement with the kinetic theory results. The shear viscosity is in good agreement with both Enskog theory and HS MD at lower densities; see Fig. 2. At the highest densities the shear viscosity of the CBA shows better agreement with HS MD than does Enskog theory. For the thermal conductivity good agreement with HS MD is found at all densities; see Fig. 3.

The self-diffusion coefficient can be represented by $D = D_E + aD_0$, where D_E is the self-diffusion coefficient for HS in the Enskog approximation [12] and $D_0 = \sigma^2\Gamma/6$ is the self-diffusion coefficient for a random walker in three dimensions with jump rate Γ and step length σ. The value of aD_0, nonexisting in the Enskog

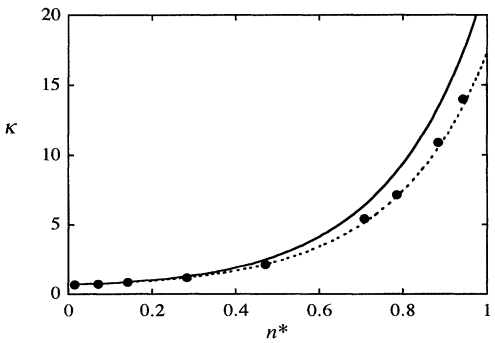

FIG. 3. HS thermal conductivity as a function of number density (with $kT = m = \sigma = 1$, $n^* = n\sigma^3$). The solid curve represents CBA, the dashed curve Enskog theory, and the solid circles HS MD (from [11]).

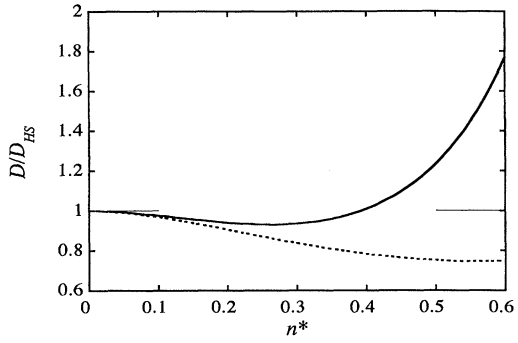

FIG. 4. HS self-diffusion (normalized by MD self-diffusion) as a function of number density. The solid curve represents CBA and the dashed curve Enskog theory.

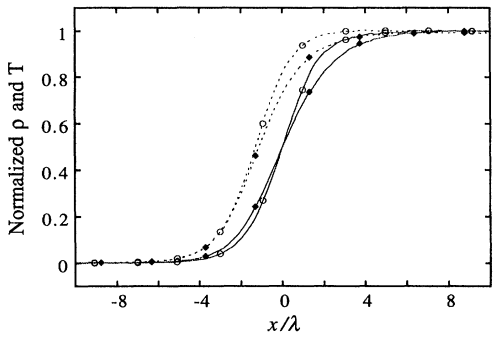

FIG. 5. Density (solid curves) and temperature (dashed curves) versus normalized position for a Mach 2 shock wave. The total shock tube length is 70 mean free paths (70λ), the upwind number density is $n^* = 0.1$, and the downwind density, determined from Hugoniot conditions, is $n^* = 0.187$ for CBA and $n^* = 0.229$ for DSMC. CBA is represented by filled symbols, standard DSMC (with Y factor enhanced collision rate) open symbol.

theory, can be derived from $A = 1$, $B = -4\pi/3(3\sqrt{3} + \pi)$, and the numerically determined value of $s \approx 0.628 \pm 0.001$. The numerical value of $a = 0.200 \pm 0.001$ is less than 1 because of negative correlation between successive displacements (i.e., $B < 0$). This self-diffusion coefficient is in better agreement with HS MD than Enskog theory for number densities up to $n\sigma^3 \equiv n^* \approx 0.5$; see Fig. 4. At higher densities the agreement fails because the displacement becomes of greater magnitude than the mean free path. The self-diffusion is also too large at higher densities because backscattering events connected with structural effects are absent in this model (i.e., there is no "caging").

The CBA runs with nearly the same efficiency as standard DSMC at low densities, since the calculation of displacements and the use of the Y factor only increase the computational cost by a few percent. At low densities HS MD is inefficient because of the large number of possible collision partners within a neighborhood of a mean free path [13]. Thus, the number of operations per collision per particle with HS MD goes as n^{-2} at low densities, while it is independent of density for CBA. In comparison with a scalar HS MD code the CBA runs 2 orders of magnitude faster for $n^* = 0.01414$. This advantage can be further enhanced by running on a parallel architecture [14].

At high densities the CBA becomes inefficient compared with HS MD. The reason is that a cell the size of a mean free path, for example, one which is roughly 1/10 of a HS diameter, represents only a small fraction (1/1000) of a single HS particle. Thus 20×10^6 particles are required to represent 1000 HS particles, assuming 20 particles per cell. On a single processor computer HS MD and CBA are of comparable efficiency at $n^* \approx 0.3$, while on a massively parallel machine (with 1000 processors) this "break-even" density increases to $n^* \approx 0.7$.

In conclusion, DSMC has been a popular method for the simulation of aerodynamic flows where conventional Navier-Stokes solvers are inaccurate. The CBA will extend its applicability to a variety of new problems that involve moderate density gases. These include the study of cold boundary layers in high altitude flows and dense shocks [15,16]. As an example, the normalized density and temperature profiles for a Mach 2 shock wave [17] are compared in Fig. 5 to the profiles obtained from standard DSMC. The methodology described in this Letter can be extended to more realistic intermolecular potentials by varying the displacement as a function of density and temperature. The implementation of such an extension is in progress.

We thank Wm. Crutchfield, G. L. Eyink, A. J. C. Ladd, M. Malek Mansour, M. Mareschal, and T. E. Wainwright for a number of very helpful discussions and J. B. Bell for support. This work was carried out under the auspices of the Department of Energy at Lawrence Livermore National Laboratory under Contract No. W-7405-ENG-48.

*Permanent address: Department of Physics, San Jose State University, San Jose, CA 95192-0106

[1] G. A. Bird, *Molecular Gas Dynamics and the Direct Simulation of Gas Flows* (Clarendon, Oxford, 1994).

[2] A. L. Garcia, *Numerical Methods for Physics* (Prentice Hall, Englewood Cliffs, NJ, 1994), Chap. 10.

[3] W. Wagner, J. Stat. Phys. **66**, 1011 (1992).

[4] M. P. Allen and D. J. Tildesley, *Computer Simulation of Liquids* (Clarendon, Oxford, 1987).

[5] Modified collision rates are commonly used in DSMC to reproduce the transport properties of nonhard sphere gases, e.g., of Maxwell molecules and of the variable hard sphere model [1]. However, these modifications retain the ideal gas equation of state. See also F. Baras, M. M. Mansour, and A. L. Garcia, Phys. Rev. E **49**, 3512 (1994).

[6] P. Resibois and M. De Leener, *Classical Kinetic Theory of Fluids* (John Wiley and Sons, New York, 1977).
[7] Note that the Landau-Boltzmann equation also includes particle interactions by modifying the advection. See L. D. Landau, Sov. Phys. JETP **3**, 920 (1957); S. Grossmann, Il Nuovo Cimento **37**, 698 (1965).
[8] F. J. Alexander, A. L. Garcia, and B. J. Alder, in *25 Years of Non Equilibrium Statistical Mechanics,* edited by J. Brey, J. Marro, M. Rubi, and M. San Miguel, Lecture Notes in Physics (Springer-Verlag, Berlin, 1995).
[9] Moving to contact, *each* point particle travels an extra distance $\sigma/2$ (as compared with hard rods). Moving apart after the collision, each point particle must also travel an additional distance $\sigma/2$.
[10] T. E. Wainwright, J. Chem. Phys. **40**, 2932 (1964).
[11] B. J. Alder, D. M. Gass, and T. E. Wainwright, J. Chem. Phys. **53**, 3813 (1970).
[12] J. J. Erpenbeck and W. W. Wood, Phys. Rev. A **43**, 4254 (1991).
[13] M. Reed and K. Flurchick, Comput. Phys. Commun. **81**, 56 (1994).
[14] M. A. Fallavollita, J. D. McDonald, and D. Baganoff, Comp. Sci. Eng. **69**, 269 (1992).
[15] E. Salomons and M. Mareschal, Phys. Rev. Lett. **69**, 269 (1992).
[16] A. Frezzotti and C. Sgarra, J. Stat. Phys. **73**, 193 (1993).
[17] The Mach number for the shock wave is defined as the upwind fluid speed divided by the sound speed in the upwind gas.